machines

MDPI

*Article*

# Physics-Informed Digital Twin of a Milling System for Vibration Prediction and Surface Roughness Modeling

**Muhamad Aditya Royandi [1], Wei-Zhu Lin [2], Jui-Pin Hung [3,*], Yu-Sheng Lai [3] and Zheng-Mou Su [3]**

[1] Department of Manufacturing Design Engineering, Politeknik Manufaktur Bandung, Bandung 40135, Indonesia; aroyandi@de.polman-bandung.ac.id
[2] Department of Mechanical Engineering, National Chin-Yi University of Technology, Taichung 411030, Taiwan; weichu80131@ncut.edu.tw
[3] Graduate Institute of Precision Manufacturing, National Chin-Yi University of Technology, Taichung 411030, Taiwan; sla9t1001@student.ncut.edu.tw (Y.-S.L.); sla8t1002@student.ncut.edu.tw (Z.-M.S.)
* Correspondence: hungjp@ncut.edu.tw; Tel.: +886-4-2392-4505 (ext. 7181); Fax: +886-4-2392-571

**Abstract**

The application of digital twin (DT) technology to intelligent machining shows promise, but its effectiveness in predicting vibration and assessing surface quality has not been thoroughly validated for widespread industrial use. This study presents a physics-informed predictive digital twin framework operating in an offline or near-real-time predictive configuration for vibration prediction and surface roughness modeling in milling processes. Impact hammer testing was conducted to extract the dominant modal properties of the spindle–tool assembly, which were embedded into a Simulink-based dynamic framework to predict tool vibration under varying cutting conditions. Full-immersion slot milling experiments on AL6061 were performed for validation. Within all datasets, including training phase and validation phase, the predicted vibration amplitudes exhibit a coefficient of determination $R^2 = 0.94$ with measured values. The overall MAPE and RMSE are about 10.39% and 0.234, respectively. Power-law regression-based surface roughness prediction models were subsequently established using cutting parameters and both measured and DT-predicted vibration features through logarithmic transformation and least-squares fitting. The results show that the roughness prediction model using vibration features predicted by the digital twin model achieved a correlation coefficient of approximately $R^2 = 0.84$, with MAPE = 9.57% and RMSE = 0.16 μm, which is comparable to the predictive model based on experimentally measured vibration. These results indicate that, within the investigated machining conditions, the digital twin can provide vibration features suitable for surface roughness prediction, demonstrating its potential as a virtual sensing approach. This work advances digital twin applications from process monitoring toward predictive, quality-oriented machining systems and provides a foundation for adaptive parameter updating in intelligent manufacturing environments.

**Keywords:** digital twin; milling dynamics; machining vibration; physics-informed modeling; surface roughness modeling



Academic Editors: Huitian Lu, Mohammad Omidi and Ali Naderi Bakhtiyari

Received: 21 April 2026
Revised: 15 May 2026
Accepted: 19 May 2026
Published: 21 May 2026



## 1. Introduction

In Industry 4.0, the digitalization of the manufacturing system has emerged as one of the important strategies to improve the productivity of the CNC machine tool and minimize operating costs [1]. Digital twin and virtual manufacturing have been widely recognized and emphasized in the Industry 4.0 era because they provide the possibility to predict

the behavior of the system and optimize the process according to the changing needs of the production process [2]. A digital twin was initially defined as a digital replica of a physical asset that provides the possibility to replicate the whole lifecycle of the system [3]. In general terms, digital twin technology establishes the connection between the physical and digital worlds and helps to eliminate uncertainties and restrain unexpected behavior in complex manufacturing environments [4]. The DT of the production system is considered as a virtual prototype with computation and prediction capabilities that can create real-time behavior through data-driven virtual replicas of physical systems for monitoring, prediction, and optimization [5]. Because current prediction methodologies predominantly depend on historical data and empirical models, the continuous exchange of data is crucial for upholding prediction accuracy. To mitigate this, Li et al. [6] proposed a digital twin framework to facilitate bidirectional interaction between physical and virtual systems. This can thereby help to update real-time models to support decision-making and processes optimization. Furthermore, this functionality is expanded to a multi-view framework, which allows for the precise prediction of energy efficiency across various levels of the machining system [6].

In the machine industry, DT models are mainly applied in product design optimization, process development, and production monitoring [4,7–9]. During the early design stage, these models utilize historical data to conduct quantitative analysis and improve design decisions. In addition, application-oriented DT models have been developed for machining quality and process [10,11]. By combining machine tool dynamics with process parameters, DT models can simulate machining processes in detail and help identify potential issues before actual production [12,13]. Another important feature of DT technology is its ability to combine physical modeling with data-driven approaches across different stages of the product lifecycle. As manufacturing systems become more complex, the collection and analysis of machining data from CNC machine tools are increasingly necessary, since these systems directly influence overall production performance [14,15]. To support this, Tao et al. [16] proposed a five-dimensional DT framework consisting of physical entity, virtual entity, service system, digital twin data and connection. This framework has been widely adopted in subsequent studies. This concept also enables the development of digital twin models to provide a convenient way to simulate machining processes in a virtual environment [13,17]. Liu et al. [13] utilized a multidimensional model (MDTMM) with integration of the physical equipment, high realistic virtual entities, and a fused data layer to enable real-time mapping between the workshop floor and the digital space. The digital twin model was used to analyze system behavior when abnormal conditions occur, based on synchronized data from the physical system, hence yielding significant performance improvements. Bakhshandeh et al. [17] developed a digital-twin-assisted monitoring system that fuses virtual cutter–workpiece engagement (CWE) maps with real-time CNC sensory data. This DT system enables adaptive control of cutting loads and provides a robust mechanism for tool condition monitoring and chatter avoidance by reconstructing physical process states in a cyber–physical environment. However, accurately reproducing real machining dynamics remains a challenging task. In practice, this requires not only real-time sensing data, such as cutting force and vibration state, but also appropriate integration with process knowledge [12]. In this respect, data-driven approaches play an important role in connecting the physical system with the digital module, enabling monitoring and optimization of manufacturing processes [18].

As known in practical machining environments, system performance depends on both machine conditions and process parameters, including system dynamics, operational status, and management-related factors [7–9]. During milling, the dynamic characteristics of the milling tool system are complex with time-varying characteristics. As a result, tool

vibration becomes a key factor influencing machining quality and tool wear. Previous studies have shown that machining vibration is closely related to cutting parameters and machine dynamics, and therefore it is often used as an indicator for evaluating machining performance [12,19,20]. Cai et al. [12] proposed a DT-based framework that integrates multiple sensing signals with process information. Their studies verified that the surface roughness can be related to spindle current and vibration signals, which improves prediction capability during operation. Qiu et al. [20] presented a structural-dynamics-driven digital twin model to simulate real-time machine vibrations by integrating self-excitation modal parameters from servo motors with finite-element-based dynamic responses. Experimental results indicated that the twinned vibration data is well correlated with surface roughness, which shows that a dynamics-driven digital twin system can work as a virtual sensor for real-time chatter detection and surface quality control.

Current research in machining monitoring mainly focuses on predicting machining quality, including surface roughness, tool vibration, and tool wear behavior. Some analytical models have been proposed for surface roughness estimation [21–23], tool wear monitoring [24–27], and vibration modeling [28–30]. However, many studies rely on data-driven approaches, where experimental data and process parameters are used to develop regression or machine learning models [28–31]. Although these models can achieve good accuracy under specific conditions, their applicability is often limited when the operating conditions change. Chen et al. [30] developed a surface roughness prediction model using a nested ANN approach with consideration of cutting force and vibration signals, while Lin et al. [19] established a surface roughness predictive model by combining the vibration features and cutting parameters in regression analysis and artificial neural network modeling. These results indicate that incorporating vibration information can improve prediction accuracy compared with models based only on process parameters. Qiao et al. [31] presented a digital-twin-based approach for predicting machining tool condition, in which physical systems, virtual models, and data analytics were integrated into a unified framework. Their experimental results showed that the proposed method is capable of predicting tool wear with good accuracy under varying machining conditions, thereby supporting predictive maintenance. Zhao et al. [32] developed a finite-element-based digital model of a lathe, where the dynamic behavior of the feed system was identified using vibration features obtained from experiments. The model not only represents the dynamic characteristics of the machine tool but also incorporates a cutting force model to predict force variations during machining.

Chatter is another important issue in machining, as it can significantly affect machining accuracy and tool life. For this reason, considerable attention has been devoted to its prediction and suppression. The prediction and suppression of chatter rely mainly on cutting force models [33,34]. However, the accuracy of these models is influenced by several factors, including tool geometry, material properties, and contact conditions [35]. In addition, the interaction between the cutting edge and the machined surface can introduce damping effects, such as friction damping and process damping [36,37]. These effects have been demonstrated to have significant influence on system dynamics but make stability prediction more difficult [38–40]. In addition, signal-based methods using force and vibration measurements have been widely applied to monitor machining processes [41–44]. In a different approach, Afazov et al. [44] proposed a digital twin model that directly uses measured cutting forces to estimate vibration behavior, instead of relying on traditional force models. This method allows real-time detection of chatter and provides a way to improve process stability.

Despite the significant progress in digital twin (DT) frameworks for CNC machining, several limitations remain. Many digital twin models depend heavily on measured signals,

which limits their use in situations where sensor data is not readily available. Existing digital twin studies in machining can generally be categorized into physics-based structural dynamics frameworks and sensor-fusion/data-driven approaches. Structural-dynamics-oriented DT models primarily focus on chatter prediction, stability analysis, or vibration response simulation, while sensor-fusion DT frameworks emphasize process monitoring using experimentally measured signals and machine learning techniques.

To address this gap, the present study proposes a physics-informed digital twin framework that integrates structural dynamics, mechanistic cutting force excitation, and calibrated process damping within a unified time-domain simulation environment. In addition, the predicted vibration features generated by the digital twin are directly utilized for surface roughness prediction, enabling a linkage between physics-based vibration prediction and machining quality assessment. In addition, limited attention has been given to process damping effects, which are not always fully incorporated into DT frameworks. Furthermore, vibration prediction and surface roughness modeling are often treated separately, without a unified approach that links machining dynamics to surface quality prediction, which can be solved by utilizing DT-predicted vibration responses directly for machining quality prediction.

In the present study, AL6061 and full-immersion slot milling conditions were selected as the validation case because they provide stable machining characteristics, well-documented cutting behavior, and relatively strong continuous cutting excitation, which facilitate clearer observation of machining vibration, process damping effects, and vibration-induced surface generation mechanisms. Unlike purely data-driven approaches, the model incorporates the dynamic characteristics of the milling tool system together with cutting force formulations that include regenerative and process damping effects.

A systematic calibration methodology is proposed to identify process damping coefficients based on experimental vibration data, and an explicit parametric model is established to describe the variation in process damping with cutting conditions. Furthermore, the developed digital twin model is used to predict tool vibration under different machining conditions, and the predicted vibration features are incorporated into a surface roughness prediction model together with cutting parameters. In this framework, the data-driven layer is physically informed through vibration features generated by the mechanistic dynamic simulation rather than relying solely on experimentally measured signals or purely empirical relationships. The regression-based surface roughness model therefore remains connected to physically interpretable machining dynamics, including structural modal behavior, regenerative vibration effects, and process damping characteristics embedded within the digital twin formulation.

The results demonstrate that the digital-twin-generated vibration signals can effectively replace experimentally measured signals, achieving comparable prediction accuracy for surface roughness. This confirms the capability of the digital twin as a virtual sensing tool for machining quality prediction. Finally, the contributions are summarized as follows: (1) A physics-informed digital twin framework for milling operations was developed by integrating structural dynamics, mechanistic cutting force modeling, and process damping within a time-domain simulation environment. (2) A structured calibration methodology was established to identify process damping coefficients under varying cutting conditions, enabling improved prediction of machining vibration responses. (3) The DT-model-predicted vibration responses were further utilized as virtual sensing features for surface roughness prediction, thereby establishing a direct linkage between physics-based vibration prediction and machining quality assessment. (4) The proposed methodology provides a physically interpretable approach for predictive monitoring and virtual sensing in intelligent machining systems, offering potential for future adaptive machining applications.

## 2. Establishment of the Digital Twin Model

### *2.1. Overview of the Digital Twin Modeling Framework*

The proposed digital twin (DT) of the milling system integrates structural dynamics, mechanistic cutting force modeling, regenerative chatter formulation, and process damping calibration within a unified time-domain simulation framework. The DT is constructed to predict tool-tip vibrations under varying cutting parameters and to provide physically consistent input for surface roughness modeling.

The modeling procedure consists of:

1. Identification of modal parameters of the milling tool system through impact testing.
2. Formulation of a two-dimensional (2-DOF) dynamic milling model.
3. Implementation of a mechanistic cutting force model including shear and edge force components and process damping effect.
4. Incorporation of regenerative time-delay effects.
5. Modeling and calibration of process damping.
6. Time-domain numerical integration for vibration prediction and validation.
7. Establishment of the surface roughness prediction model based on predicted vibration features.

Although the surface roughness prediction layer employs regression-based statistical modeling, its input variables are not derived solely from empirical measurements. Instead, the regression model utilizes vibration features generated by the mechanistic digital twin simulation, which incorporates experimentally identified modal dynamics, regenerative vibration effects, and calibrated process damping behavior. Therefore, the statistical prediction layer remains physically connected to the underlying machining dynamics through the physics-based vibration simulation framework. This integration preserves the physical interpretability and dependability of the overall digital twin system while enabling practical surface quality prediction under varying machining conditions.

### *2.2. Dynamics of the Machining Process*

The dynamic behavior of a machining system can be represented by an equivalent mechanical model. For simplicity, the milling system is initially modeled as a one- or two-degree-of-freedom structure in the feed (x) and normal (y) directions, as illustrated in Figure 1. For a one-degree-of-freedom system, the structural dynamics are characterized by the equivalent mass $m$, stiffness $k$, and damping coefficient $c$. The dynamic force equilibrium at the tool tip is expressed as

$$m\ddot{x}(t) + c\dot{x}(t) + kx(t) = F(t) \tag{1}$$

where $x(t)$ denotes the relative displacement between the tool and workpiece, and $F(t)$ represents the time-varying cutting force.

Essentially, the cutting force originates from the resistance encountered at the tool–workpiece interface and is proportional to the instantaneous uncut chip area. Considering the regenerative mechanism induced by vibration in the feed direction, the chip thickness becomes dependent on both the current and previous tool positions. Consequently, the dynamic cutting force can be expressed as

$$F(t) = K_f a_p [h_0 + x(t) - x(t - T)] \tag{2}$$

where $K_f$ is the cutting force coefficient in the feed direction, $a_p$ is the axial depth of cut, $h_0$ denotes the nominal feed per revolution, and $T$ represents the tooth passing period. The term $x(t) - x(t - T)$ captures the regenerative effect responsible for self-excited vibration (chatter).

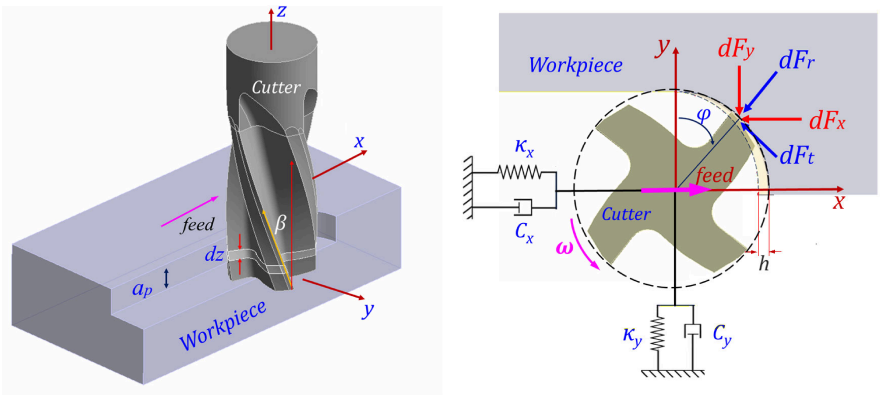


**Figure 1.** Machining system with two degrees of freedom.

Considering process damping effects on vibration suppression, the process damping force was introduced into the dynamic cutting force equation based on studies by Chen et al. [30], which can be expressed as

$$F_{pd} = (C_{pd}\frac{ah}{V_c})\dot{x}(t) = C_{eff}\dot{x}(t) \tag{3}$$

It is noted that the process damping force is directly proportional to both the cutting width and vibration velocity, while it maintains an inverse relationship with the cutting speed [21,22]. $V_c$ is the cutting speed and $C_{pd}$ is the process damping coefficient, which characterizes the contact interaction between the flank face and the undulated workpiece surface. This coefficient is typically identified experimentally through dynamic cutting tests. $C_{eff}$ represents the effective damping coefficient.

By incorporating both regenerative cutting force and process damping force, the dynamic equation becomes

$$m\ddot{x}(t) + \left(c + \frac{C_{pd}a_p h_0}{V_c}\right)\dot{x}(t) + kx(t) = K_f a_p[h_0 + x(t) - x(t-T)] \tag{4}$$

$$m\ddot{x}(t) + \left(c + C_{eff}\right)\dot{x}(t) + kx(t) = K_f a_p[h_0 + x(t) - x(t-T)] \tag{5}$$

The additional damping term enhances system stability, particularly under low cutting speed conditions. This mechanism increases the critical depth of cut and enlarges the chatter-free stability region. For more realistic representation, the system can be extended to a two-dimensional (2-DOF) dynamic model, as shown in Figure 1. In this formulation, vibration components in both the feed and normal directions are considered, allowing improved prediction accuracy of tool-tip dynamics and cutting force variations.

$$\mathbf{M}\ddot{\boldsymbol{X}}(\boldsymbol{t}) + C\dot{\boldsymbol{X}}(\boldsymbol{t}) + \boldsymbol{k}\boldsymbol{X}(\boldsymbol{t}) = \boldsymbol{F_c}(\boldsymbol{t}) - \boldsymbol{F_{pd}}(\boldsymbol{t}) \tag{6}$$

where $\boldsymbol{F_c}(\boldsymbol{t})$ is the cutting force vector and $\boldsymbol{F_{pd}}(\boldsymbol{t})$ is the process damping force vector.

$$\mathbf{M} = \begin{bmatrix} m_x & 0 \\ 0 & m_y \end{bmatrix}, \mathbf{C} = \begin{bmatrix} c_x & 0 \\ 0 & c_y \end{bmatrix}, \mathbf{K} = \begin{bmatrix} k_x & 0 \\ 0 & k_y \end{bmatrix} \tag{7}$$

In the above, $m_x$ $m_y$; $k_x$ $k_y$ and $c_x$ $c_y$ are the equivalent mass, structural stiffness and structural damping in the X and Y directions.

The local cutting force components $(dF_x, dF_y)$ acting on the cutting edge engaged with the workpiece with a differential axial depth $dz$ in the X and Y directions can be expressed as follows [45]:

$$dF_x = -dF_t sin\varphi + dF_r cos\varphi \tag{8}$$

$$dF_y = -dF_t cos\varphi + dF_r sin\varphi \tag{9}$$

where $dF_t$ and $dF_r$ are the infinitesimal local cutting forces in the tangential and radial directions, respectively, and φ represents the immersion angle of cutting edge.

$$dF_t = K_{tc} h dz + K_{te} dz / cos\beta \tag{10}$$

$$dF_r = K_{rc} h dz + K_{re} dz / cos\beta \tag{11}$$

where $K_{tc}$ and $K_{rc}$ are the shear force coefficients in the tangential and radial directions, respectively; $K_{te}$ and $K_{re}$ are the tangential and radial edge force coefficients, respectively; and β is the helix angle of the cutting edge of the tool.

The total cutting force is obtained by summing contributions from all engaged teeth and axial slices. Helical geometry is incorporated through axial discretization and angular phase shift along the flute. Also, the inclusion of edge force coefficients is particularly important under small chip thickness conditions, where ploughing effects significantly influence dynamic excitation.

In addition, the regenerative mechanism arises from the interaction between the current tooth and the surface left by the previous tooth. The instantaneous uncut chip thickness for each tooth is given by

$$h(\varphi, t) = f_z sin\varphi + [x(t) - x(t-T)]sin\varphi - [y(t) - y(t-T)]cos\varphi \tag{12}$$

where $f_z$ is the feed per tooth and φ is the angular position of the cutting edge.

To accurately reflect the physical behavior of the machining system, the key dynamic parameters—equivalent mass, structural stiffness, and damping—must be identified experimentally. Modal testing or impact hammer tests are typically employed for parameter extraction. Once calibrated, the dynamic model enables prediction of cutting forces and tool vibrations under varying machining conditions. The prediction results can be used to adjust cutting parameters, reduce vibration and tool wear, and improve cutting quality.

### *2.3. Dynamic Characteristic and Modal Parameters*

To accurately capture the structural behavior of the milling machine, modal analysis was performed from the results of vibration tapping tests. The dynamic characteristics of the milling system are represented by its natural frequencies, modal stiffness, and modal damping ratios. These modal parameters define the frequency response function (FRF) of the system in real and imaginary parts as shown in Figure 2, which describes the relationship between dynamic excitation forces and structural displacement.

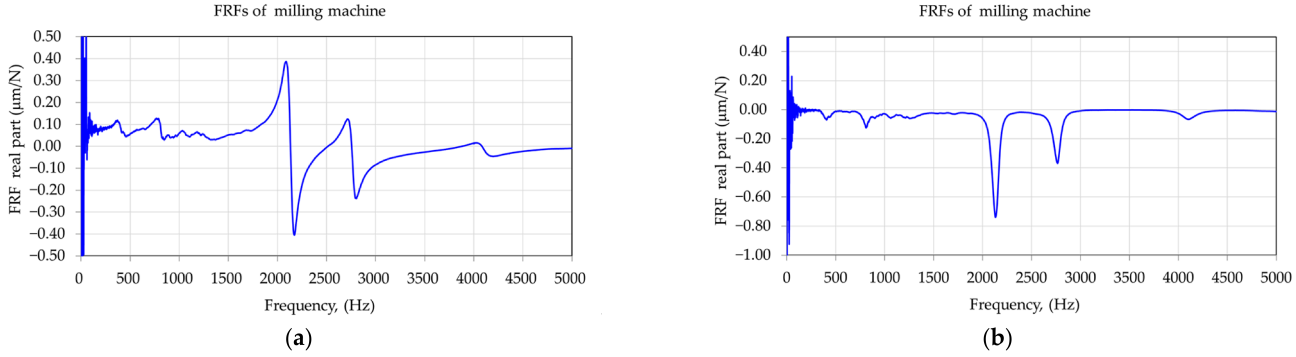


**Figure 2.** Typical frequency response function of the milling tool. (**a**) Real part; (**b**) imaginary part.

The frequency response function can be expressed as

$$H(\omega) = \frac{X(\omega)}{F(\omega)} = \frac{1}{k - m\omega^2 + jc\omega} \tag{13}$$

where $\omega$ denotes the excitation frequency, and $m$, $c$, and $k$ represent the equivalent modal mass, damping, and stiffness, respectively.

In practice, the modal parameters are identified experimentally through impact hammer testing or operational modal analysis. The measured response signals are processed to extract (1) natural frequency $\omega_n$, (2) modal damping ratio $\zeta$ and (3) modal stiffness $k$. These experimentally identified parameters ensure that the dynamic model accurately reflects the physical system rather than relying on idealized assumptions.

### *2.4. Calibrating the Process Damping Characteristics*

Process damping plays an important role in determining the vibration amplitude of milling operations. Unlike structural damping, which is determined by the inherent dynamic properties of the machine tool system, process damping depends strongly on cutting conditions such as axial depth of cut, feed per tooth, and cutting speed [36]. Therefore, an appropriate calibration procedure is required to determine the effective process damping coefficient used in the digital twin model. In this study, the process damping coefficient $C_{pd}$ was identified by matching the predicted vibration responses of the milling dynamic model with experimentally measured vibration signals under different cutting conditions. For each machining test, the time-domain milling dynamic simulation was performed using the identified structural parameters and mechanistic cutting force coefficients. The predicted tool-tip acceleration was then compared with the measured acceleration signal obtained from the accelerometer mounted on the spindle housing. The root mean square (RMS) value of the acceleration was used as the primary metric for comparison.

For a given cutting condition defined by spindle speed $n$, axial depth of cut $a_p$, and feed per tooth $f_z$, the value of $C_{pd}$ was iteratively adjusted until the simulated vibration amplitude approached the experimentally measured RMS vibration level.

Let $a_{RMS}^{exp}$ denote the measured RMS vibration acceleration and $a_{RMS}^{sim}$ denote the predicted RMS vibration obtained from the digital twin simulation. The calibration of $C_{pd}$ was performed by minimizing the relative error between these two quantities, defined as

$$\varepsilon = \frac{|\, a_{RMS}^{sim} - a_{RMS}^{exp} \,|}{a_{RMS}^{exp}} \tag{14}$$

For each cutting condition $(n, a_p, f_z)$, the value of $C_{pd}$ was iteratively adjusted until the error $\varepsilon$ reached a minimum. In practice, the calibration procedure aimed to achieve a relative error within an acceptable tolerance band, typically below 5~10%. When this condition was satisfied, the resulting calibrated values of $C_{pd}$ represent the effective process damping contribution required for the dynamic model to reproduce the observed vibration behavior.

## 3. Overview of the Digital Twin Framework

The digital twin developed in this study is designed as a physics-informed predictive framework that synchronizes the physical machining process with its computational counterpart. Unlike purely data-driven approaches, the proposed architecture integrates experimentally identified structural dynamics with a mechanistic cutting force model to enable reliable prediction of machining vibration and surface quality.

The digital twin serves two primary objectives:

1. Prediction of tool vibration under varying cutting conditions.

2. Prediction of surface roughness through integration of dynamic response and machining parameters.

The overall framework for the application of the DT model in the machining process is shown in Figure 3, including the following functions:

1. DT model based on identified system parameters.
2. Dynamic vibration prediction module.
3. Surface roughness prediction module.

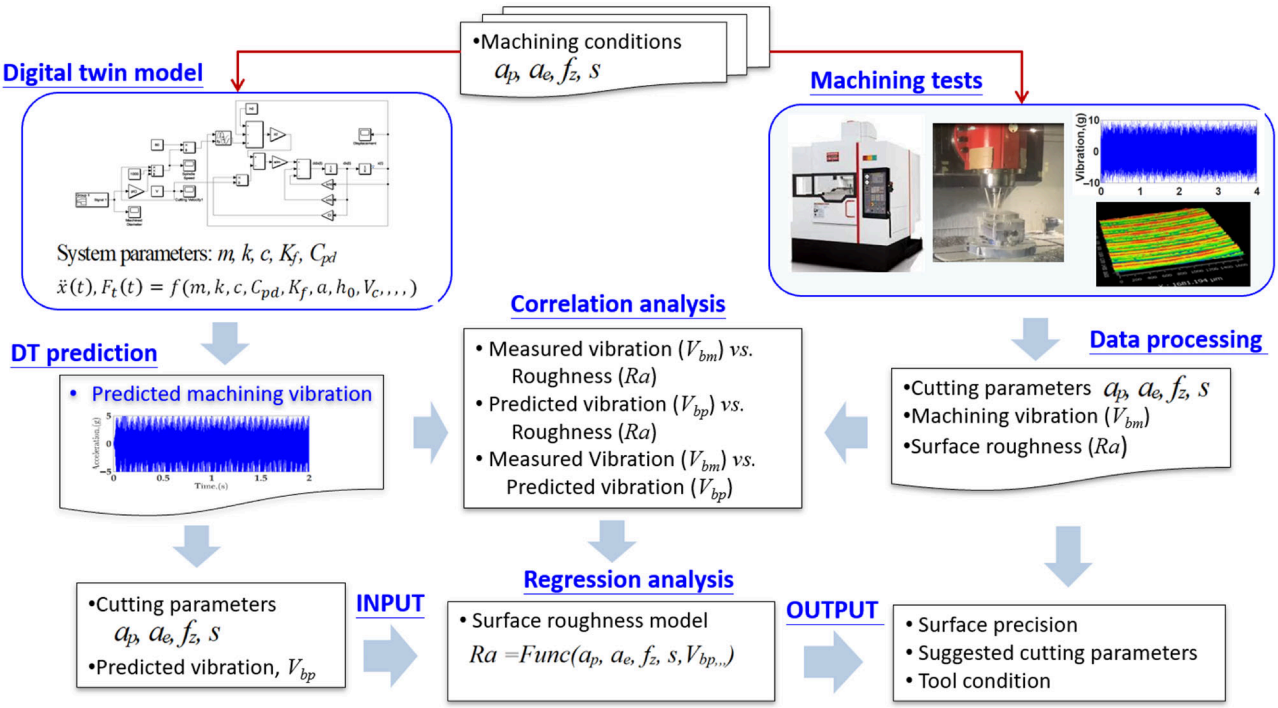


**Figure 3.** Overview of the digital twin framework and application.

### *3.1. DT Model Based on Identified System Parameters*

The structural foundation of the digital twin is established through experimental modal analysis of the spindle–tool system. Impact hammer testing is conducted to obtain the frequency response functions (FRFs), from which modal mass, stiffness, and damping parameters are identified. These experimentally determined modal parameters are embedded into the dynamic cutting force model described in Section 2.1. This ensures that the virtual model accurately reflects the real structural behavior of the machining system.

By implementing the digital twin with experimentally calibrated system parameters, the model maintains physical interpretability and reduces uncertainty associated with purely theoretical assumptions.

### *3.2. Dynamic Vibration Prediction Module*

Using the identified modal parameters and the mechanistic cutting force formulation, the digital twin predicts tool vibration responses under specified cutting conditions. The model solves the dynamic governing equations incorporating regenerative effects and process damping, producing predicted vibration responses in the time and frequency domains.

The predicted vibration signals are validated through comparison with experimentally measured vibration data obtained during machining trials. This validation confirms the accuracy and stability of the digital twin under different operating conditions.

### *3.3. Surface Roughness Prediction Module*

Beyond vibration prediction, the digital twin framework is extended to estimate surface roughness. Extensive machining experiments are conducted under varying cutting conditions to collect tool vibration signals and determine the surface roughness of the machined part.

Based on the collected dataset, surface roughness prediction models are established using: (1) cutting parameters and (2) tool vibration features as input variables, with surface roughness defined as the output variable. In addition, two modeling scenarios are considered: (1) using experimentally measured vibration data and (2) using vibration responses predicted by the digital twin model.

Regression models are developed to evaluate the relationship between dynamic response and surface generation. This dual-input strategy enables assessment of whether digitally predicted vibration can effectively replace direct vibration measurements for surface quality prediction.

The digital twin functions are now organized into a compact modular digital twin workflow, as shown in Table 1. Here is a brief description of each module's function:

**Table 1.** Compact modular digital twin workflow.

| Module Unit | Interface Type | Data Input | Data Output |
|---|---|---|---|
| Milling system + physical acquisition | Sensor-to-digital | *Cutting parameters*, $a_p$, $a_e$, $f_z$, $s$ | *Vibration raw signals* ($V_X$, $Vy$, $Vz$) *Surface roughness* ($Ra$) |
| Digital twin model + dynamic simulation | Physics-to-virtual | *System parameters* ($m$, $c$, $k$)*Tool characteristics* $K_{tc}$, $K_{rc}$, $K_{te}$, $K_{re}$ *and Cpd* *Cutting parameters* $a_p$, $a_e$, $f_z$, $s$ | *Virtual vibration response* ($V_{xDT}$) |
| Feature extraction + validation analysis | Signal-to-feature | *Measured vibration signals*, ($V_X$, $V_y$, $V_z$) *Predicted vibration signals* ($V_{xDT}$) *Measured roughness* ($Ra$) | *Feature vector* [$V_{rms}$] *Determination coefficients* ($R^2$) |
| Regression analysis + quality estimation | Data-to-decision | *Combined feature vectors* [$a_p$, $a_e$, $f_z$, $s$, $V_{rms}$, $Ra$] | *Predicted roughness* ($Ra$) |

1. Milling System with Physical Acquisition Module

This unit represents the physical layer of the digital twin, responsible for executing the machining process and capturing the physical data required for model synchronization.

- Input: Machining parameters (speed $s$, feed rate $f_z$, and depth of cut $a_p$), and the physical interaction between the tool flutes and the AL6061 workpiece.
- Logic: Executes the slot milling operation on a three-axis CNC machine while utilizing high-sensitivity sensors (triaxial accelerometers and microphones) to transduce mechanical vibrations via a synchronized data acquisition (DAQ) system.
- Output: Measured high-frequency vibration signals ($V_X$, $V_y$, and $V_z$) that serve as the physical baseline for validation.

2. Digital Twin Model for Dynamic Simulation

This module serves as the predictive engine of the system. Its primary function is to simulate the tool's mechanical behavior without requiring physical contact.

- Input: Machining parameters (speed $s$, feed rate $f_z$, and depth of cut $a_p$), the experimentally identified modal parameters ($m$, $c$, and $k$) and the cutting characteristic of the cutter ($K_{tc}$, $K_{rc}$, $K_{te}$, $K_{re}$ *and* $Cpd$)
- Logic: It solves the governing equations of dynamic cutting force to create a "virtual sensing unit" of the machining process.

- Output: The DT-predicted vibration response ($V_{xDT}$), providing a high-reality estimation of tool-tip displacement.

3. Feature Extraction and Validation Module

This module acts as the system's "Reality Check." It bridges the gap between raw time-series data and statistical visualization data while ensuring the digital model remains synchronized with physical reality.

- Input: Both the measured vibration signals ($V_X$, $V_y$, and $V_z$) from physical sensors and the DT-predicted response ($V_{xDT}$).
- Logic: It converts complex signals into identifiable features, such as RMS. It then performs a statistical comparison using MAPE and correlation coefficients to validate the model's accuracy.
- Output: A validated feature vector [$V_{rms}$] that represents the true dynamic state of the cutting process.

4. Surface Roughness Prediction Module

This is the "Final Objective" of the architecture. It maps dynamic mechanical responses to surface quality and machining performance indicators.

- Input: The validated vibration feature vectors [$a_p$, $a_e$, $f_z$, $s$, $V_{rms}$, $Ra$] (derived from both the virtual and physical domains).
- Logic: Using a regression modeling approach to map the machining vibrations to the resulting surface topography.
- Output: The estimated surface roughness (Ra). This allows the system to predict the surface quality of the part being processed even if physical sensors are absent or fail.

## 4. Creation of the Digital Twin Model

### *4.1. Assessment of System Parameters of the Milling Tool*

In this section, the dynamic characteristics of the milling tool system are evaluated through impact hammer testing. The experimental setup is illustrated in Figure 4. A solid carbide milling cutter with a length of 100 mm and diameter of 12 mm was clamped in the tool holder. Two accelerometers were mounted at the tool tip along the X and Y directions to capture vibration responses in orthogonal directions.

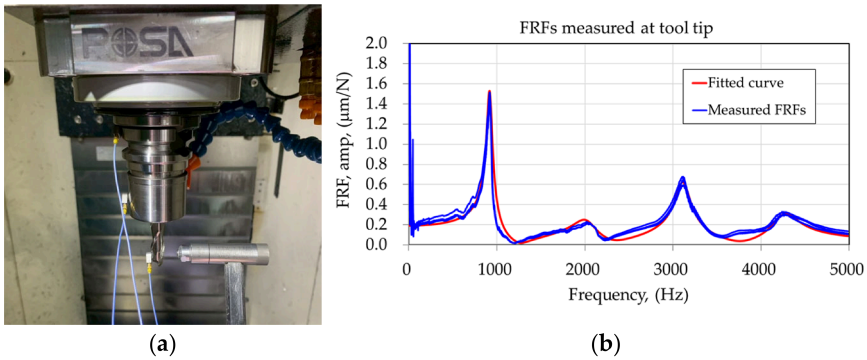


**Figure 4.** Measurement of FRF of the milling cutter. (**a**) Tapping test; (**b**) tool point FRF.

An instrumented impact hammer was used to excite the tool tip by striking it sequentially in the opposite directions corresponding to the X and Y axes. The resulting vibration responses were recorded, and the frequency response functions (FRFs) of the tool tip were obtained. The dynamic characteristics were extracted from the measured signals using Fast Fourier Transform (FFT) analysis. Based on the identified FRFs, the

modal parameters—including natural frequency, damping ratio, and dynamic stiffness associated with the dominant vibration modes—were determined.

Figure 4 illustrates the experimentally measured frequency response functions (FRFs) of the milling tool–spindle system with repeated tests. A prominent resonance peak is observed at approximately 920 Hz, corresponding to the dominant bending mode of the spindle–tool assembly. This mode exhibits the highest dynamic compliance around 1.45 μm/N and is therefore considered the principal vibration mode influencing machining stability and surface generation behavior.

The modal parameters associated with this predominant mode were identified from the measured transfer function using the curve-fitting approach described in Section 3. By fitting the analytical transfer function to the experimental FRF data, the equivalent single-degree-of-freedom (SDOF) modal parameters were extracted with satisfactory agreement between measured and reconstructed responses.

The identified system parameters, including equivalent modal mass, dynamic stiffness, and damping coefficient, are summarized in Table 2. Four sets of parameters were obtained through repeated measurements to ensure consistency and reliability. The estimated modal mass ranges from 0.201 kg to 0.272 kg, reflecting minor variation attributable to experimental uncertainty and boundary condition sensitivity. The equivalent system stiffness varies between 6690 N/mm and 9080 N/mm, while the damping coefficient falls within the range of 111–123 N·s/m. The mean values are k = 8028 N/mm, $c = 118$ Ns/m, and $m = 0.241$ kg. Since the variations were attributed to measurement uncertainty rather than changes in structural configuration, the mean values were adopted in the simulation to represent the nominal dynamic characteristics of the milling system, also serving as the fundamental input for the subsequent dynamic cutting force formulation and digital twin vibration prediction model.

**Table 2.** Modal parameters of the milling tool.

| | **Modal Stiffness [N/mm]** | **Modal Damping [N/m/s]** | **Modal Mass [kg]** |
|---|---|---|---|
| | 9080 | 117 | 0.272 |
| | 8600 | 111 | 0.258 |
| | 7740 | 121 | 0.232 |
| | 6690 | 123 | 0.201 |
| Mean value | 8028 | 118 | 0.241 |
| deviation | 1050 | 5.3 | 0.03 |

### *4.2. Establishment of the Prediction Model*

The dynamic simulation of tool vibration in the milling system was implemented using the Simulink environment in MATLAB (Version R2016a) The overall simulation structure is illustrated in Figure 5. The model integrates the dynamic cutting force formulation with the experimentally identified structural parameters of the spindle–tool assembly.

The cutting force coefficients in the tangential and normal directions were adopted from previous studies on Al-Mg-Si aluminum alloys [46] and used as reference parameters in the present work. Based on the reported values for AA6060-T6, the coefficients were taken as $K_{tc} = 745.1$ MPa and $K_{rc} = 360.98$ MPa, while the cutting-edge coefficients were $K_{te} = 31.49$ N/mm and $K_{re} = 21.85$ N/mm. Although the present machining experiments were conducted on AL6061, the adopted coefficients provided reasonable force estimation and were further validated through experimental vibration measurements and process damping calibration under the investigated cutting conditions. In addition, the process damping coefficient was determined to be $C_{pd} = 3.0 \times 10^9$ N/m$^2$, equivalent to

those reported in studies [47,48]. These coefficients were incorporated into the dynamic governing equations to characterize the excitation forces acting on the milling tool due to the damping effects.

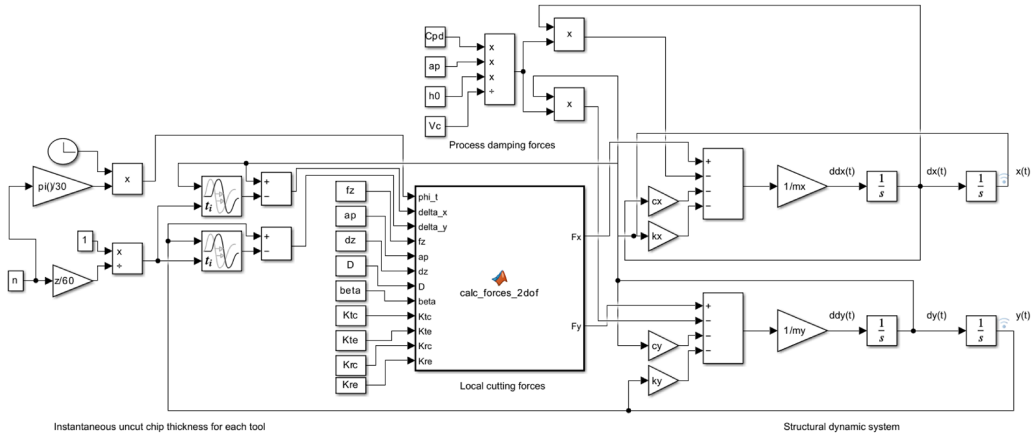


**Figure 5.** Simulink block diagram of simulation of dynamic cutting force.

The modal parameters of the milling tool system, previously extracted from impact hammer testing, were embedded into the Simulink model to represent the structural dynamics of the system. Specifically, the identified equivalent modal mass, stiffness, and damping coefficients were implemented within the vibration response block to simulate the tool-tip displacement under different machining conditions.

By integrating the calibrated cutting force coefficients with the experimentally determined structural parameters, the simulation model can be employed to predict the vibration behavior of the milling tool under different cutting conditions. This physics-based implementation ensures that the predicted vibration response reflects both process excitation characteristics and intrinsic system dynamics.

## 5. Experimental Setup and Data Acquisition

In this study, machining experiments were conducted on a CNC milling machine using a four-flute tungsten carbide end mill, as illustrated in Figure 6. The workpiece material was aluminum alloy AL 6061 with dimensions of 150 mm × 150 mm × 80 mm. Full-immersion slot milling was performed. Each slot was machined along the X direction under specific cutting parameters.

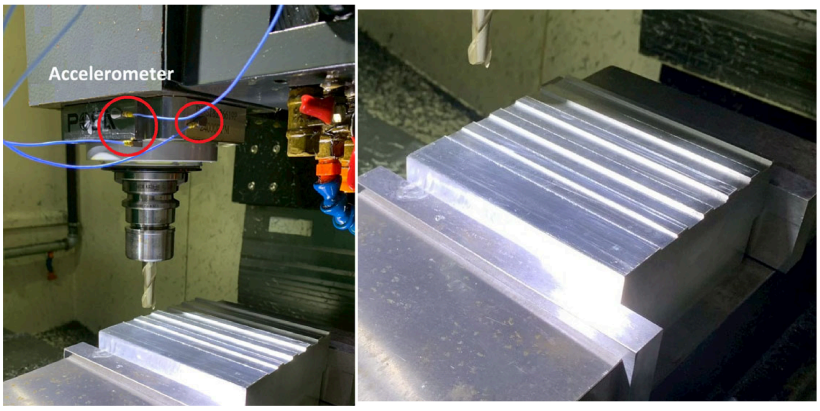


(**a**) (**b**)

**Figure 6.** Configuration of machining tests. (**a**) Accelerometer placement; (**b**) workpiece.

The machining parameters were selected to provide a representative range of milling conditions capable of generating different vibration responses, cutting force excitation levels, and process damping behaviors within the operating range of the experimental milling system. The selected spindle speeds, axial depths of cut, and feed per tooth values were intended to produce varying dynamic characteristics for calibration and validation of the proposed digital twin (DT) framework.

The machining tests were conducted in two stages. The first stage was designed to establish and calibrate the digital twin model through parameter identification and process damping calibration under different cutting conditions. In this stage, the axial depth of cut ($a_p$) was set to 1.5 mm, 2.5 mm, and 3.5 mm. The spindle speed was selected as 5500, 7500, and 9500 rpm, while the feed per tooth ($f_z$) was set to 0.05 mm/tooth, 0.075 mm/tooth, and 0.1 mm/tooth, respectively. A total of 27 machining experiments were conducted using different combinations of these cutting parameters.

The second-stage machining tests were performed to independently validate the predictive capability and generalization performance of the DT model using cutting conditions different from those employed during the calibration stage. In this validation phase, the spindle speed was varied between 3000 and 8000 rpm, while the axial depth of cut ranged from 1 mm to 4 mm. A total of 29 datasets were collected for validation of the DT model. These validation conditions were intentionally selected outside the calibration dataset to evaluate the robustness of the proposed framework under different operating conditions.

During the milling process, three single-axis accelerometers (PCB Inc., Tonawanda, NY, USA, 352A25; mass: 0.6 g; sensitivity: (±15%) 2.5 mV/g; and natural frequency: 1 to 10k Hz) were mounted on the spindle housing to measure vibration signals in the X, Y, and Z directions. For each machining test, the acceleration signals measured by the accelerometers were processed to obtain the root mean square (RMS) value of the vibration acceleration. The vibration feature RMS was selected because it represents the overall energy level of the vibration signal and is less sensitive to instantaneous fluctuations compared with peak values. In the numerical simulation, the same RMS value was calculated from the predicted acceleration response of the milling dynamic model after the transient stage had decayed.

The surface roughness measurements were obtained using a white-light interferometer (Optical Surface Profiler, Zygo NewView™ 8000 Series, ZYGO™ Middlefield, Middlefield, CT, USA) after the machining tests. The roughness values of each machined slot were measured at multiple locations along the feed direction, and the average value was used for subsequent model development.

## 6. Results and Discussions

### *6.1. Measured Vibration and Surface Morphology*

Figure 7 illustrates the tool vibration response and surface morphology of the machined surface generated under representative machining conditions. Under a spindle speed of 5500 rpm, axial depth of cut of 1.5 mm, and feed of 0.10 mm/tooth, the measured surface roughness was 1.454 μm and the average vibration level was 1.949 g. The vibration induced under machining parameters (speed 7500 rpm, cutting depth 3.5 mm, and feed 0.05 mm/tooth) is around 4.893 g with a surface roughness of 1. 81 μm. Under more aggressive cutting conditions (9500 rpm, depth of cut 3.5 mm, and feed 0.075 mm/tooth), the surface roughness increased to 1.702 μm, while the average vibration level increased to 3.927 g. As shown in Figure 7, the machining operation was conducted in a stable vibration state without significant chattering behavior. In addition, the Fast Fourier Transformation (FFT) analysis of the vibration signals show resonance at around 918~921 Hz, as illustrated in Figure 8. This confirmed that the cutting process is actively exciting the tool by the specific structural mode that appeared at 920 Hz (Figure 4b). Also, the digital twin model

established based on this critical mode can reflect structural dynamic characteristics of the milling system in operation.

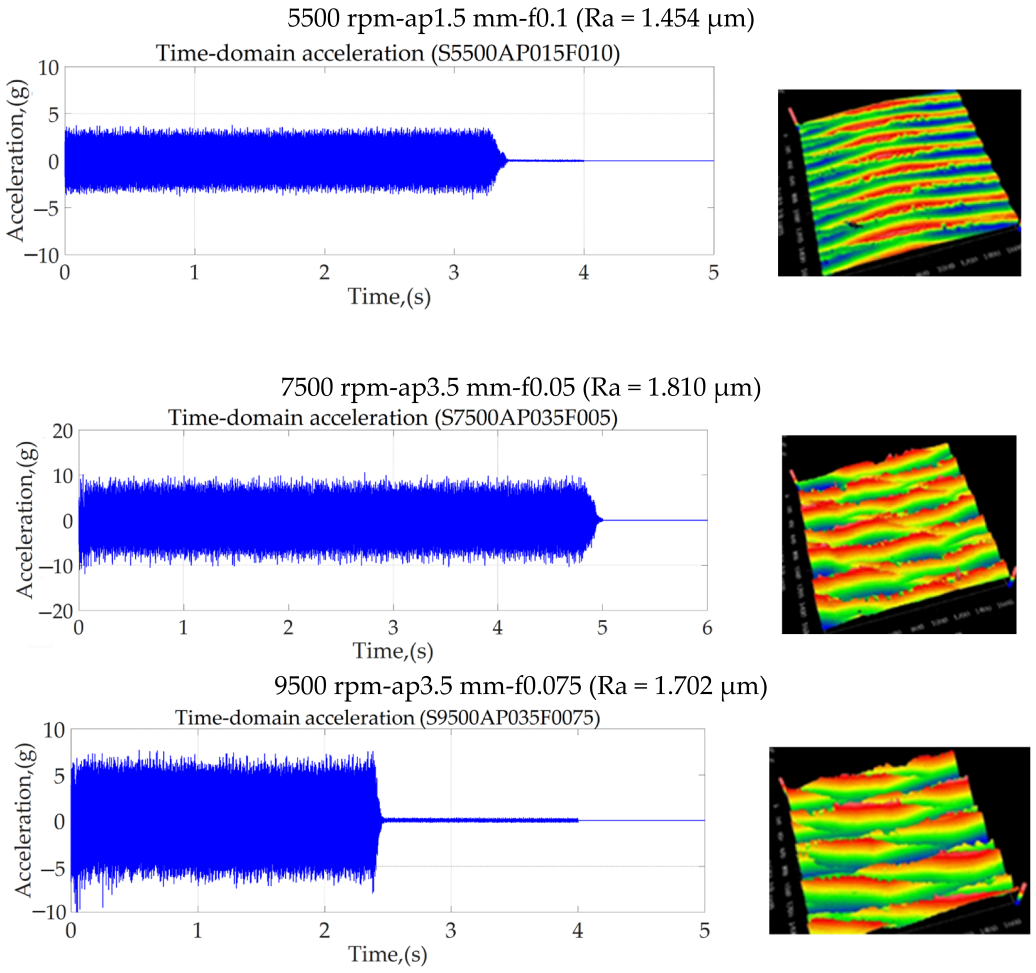


**Figure 7.** Typical vibration signal assessed at the spindle tool in the machining process and surface morphology of the machined slots.

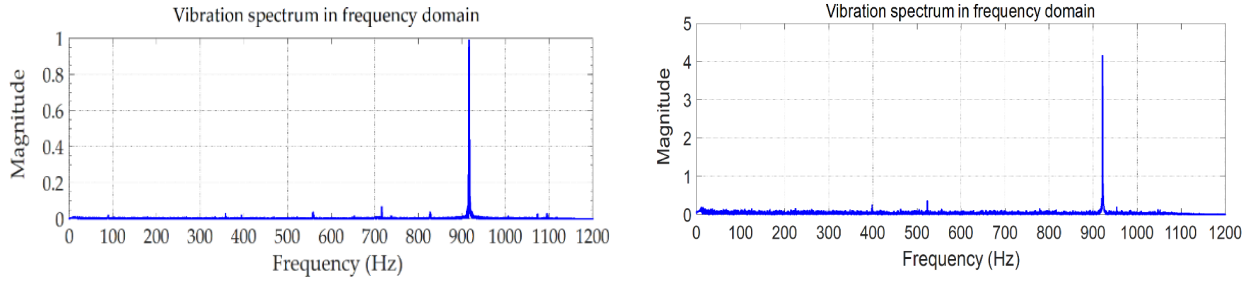


(**a**) (**b**)

**Figure 8.** Vibration spectrum in frequency domain, assessed under cutting parameters. (**a**) S5500 rpm, ap = 1.5 mm, fz = 0.01 and (**b**) S7500 rpm, ap = 3.5 mm, fz = 0.005.

### *6.2. Predicted Machining Vibration*

Figure 9 shows the typical vibration spectrum under specific conditions predicted by the digital model of the machining system. The milling tool shows consistent vibration responses as observed in machining tests. The vibration responses were predicted by the DT model implemented with the system parameters assessed from a physical milling system. In the DT model, the interactions between the cutting edge and the workpiece were characterized by cutting force resistance and process damping. The cutting forces

coefficients were obtained from previous machining tests [46], while the determination of the process damping property was a difficult task with more machining experiments. The initial values of process damping were taken from literature reports [47,48] and then were calibrated during the simulation process to ensuring the predictions under various cutting parameters approach the measurements.

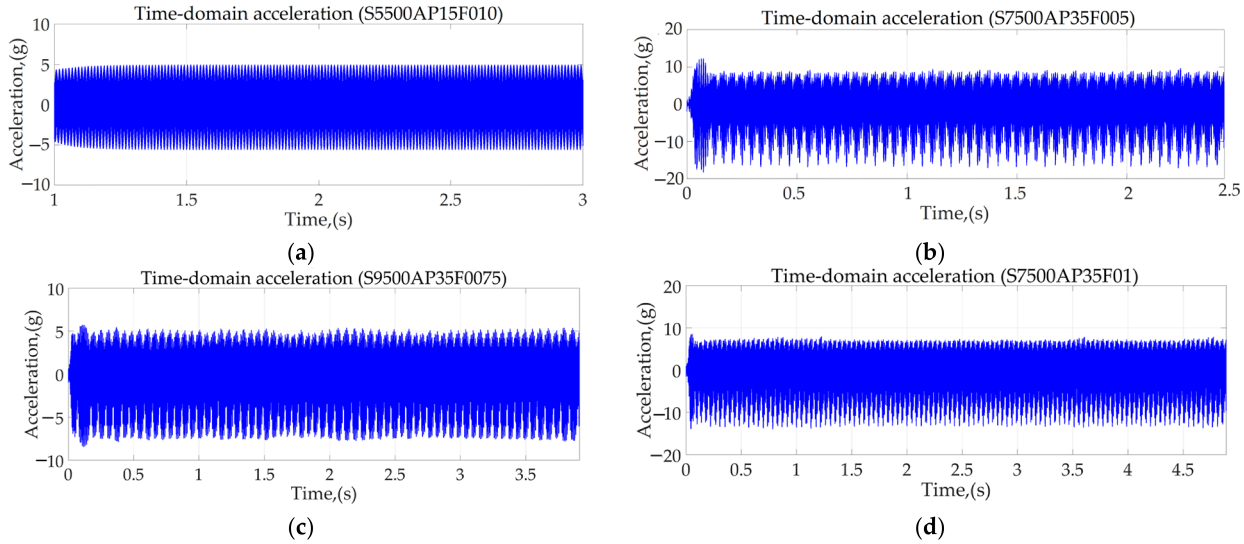


**Figure 9.** Digital-twin-model-predicted vibration spectra under specific conditions.

### *6.3. Correlation Between Measured and Predicted Vibrations*

The complete dataset obtained in first stage test is summarized in Table 3, in which the simulation results under various cutting conditions are presented for comparison with measurements. A consistent trend can be observed: increasing depth of cut and spindle speed generally leads to higher vibration amplitude, which results in an increase in surface roughness. This behavior can be attributed to intensified dynamic cutting forces and enhanced regenerative effects at higher material removal rates. As shown in Figure 10, the coefficient of determination between measured and predicted vibration amplitudes is approximately $R^2 = 0.9332$, indicating consistent predictive performance. The performance index, including root mean square error (RMSE) and mean absolute percentage error (MAPE) are 0.228 and 5.4%, respectively. Therefore, the digital twin model has been proven to possess the mechanical characteristics of real cutting systems and can reflect vibration behavior under different process parameters.

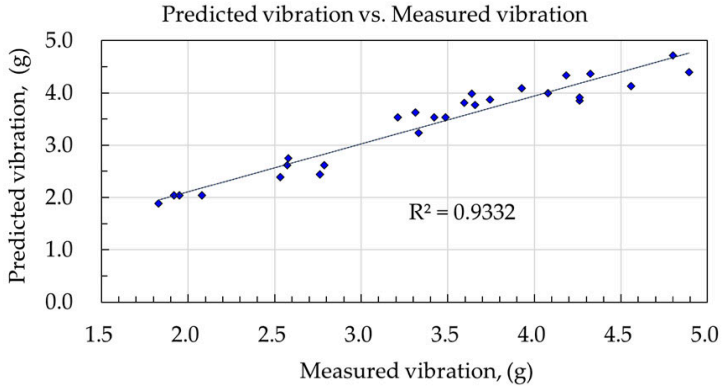


**Figure 10.** The figure of Correlation between measured and predicted vibrations.

**Table 3.** Dataset of the machining tests.

| Cutting Depth, ap (mm) | Spindle Speed, s (rpm) | Feed, fz (mm/Tooth) | Measured Vibration (g) | Predicted Vibration (g) | Roughness, Ra (μm) |
|---|---|---|---|---|---|
| 1.5 | 5500 | 0.100 | 1.949 | 2.041 | 1.454 |
| 2.5 | 5500 | 0.100 | 3.422 | 3.535 | 1.730 |
| 3.5 | 5500 | 0.100 | 3.595 | 3.810 | 2.031 |
| 1.5 | 5500 | 0.075 | 1.920 | 2.041 | 1.004 |
| 2.5 | 5500 | 0.075 | 3.210 | 3.532 | 1.298 |
| 3.5 | 5500 | 0.075 | 3.638 | 3.986 | 1.522 |
| 1.5 | 5500 | 0.050 | 2.080 | 2.041 | 1.054 |
| 2.5 | 5500 | 0.050 | 3.330 | 3.232 | 1.210 |
| 3.5 | 5500 | 0.050 | 4.260 | 3.852 | 1.342 |
| 1.5 | 7500 | 0.100 | 2.573 | 2.618 | 1.198 |
| 2.5 | 7500 | 0.100 | 3.487 | 3.532 | 2.100 |
| 3.5 | 7500 | 0.100 | 3.312 | 3.622 | 2.031 |
| 1.5 | 7500 | 0.075 | 2.762 | 2.440 | 1.169 |
| 2.5 | 7500 | 0.075 | 4.260 | 3.916 | 1.390 |
| 3.5 | 7500 | 0.075 | 4.560 | 4.126 | 1.810 |
| 1.5 | 7500 | 0.050 | 2.786 | 2.618 | 0.909 |
| 2.5 | 7500 | 0.050 | 4.183 | 4.332 | 1.256 |
| 3.5 | 7500 | 0.050 | 4.893 | 4.402 | 1.325 |
| 1.5 | 9500 | 0.100 | 2.579 | 2.749 | 1.388 |
| 2.5 | 9500 | 0.100 | 4.079 | 3.997 | 1.797 |
| 3.5 | 9500 | 0.100 | 4.799 | 4.722 | 2.122 |
| 1.5 | 9500 | 0.075 | 2.532 | 2.392 | 1.088 |
| 2.5 | 9500 | 0.075 | 3.658 | 3.767 | 1.625 |
| 3.5 | 9500 | 0.075 | 3.927 | 4.093 | 1.702 |
| 1.5 | 9500 | 0.050 | 1.830 | 1.885 | 0.763 |
| 2.5 | 9500 | 0.050 | 3.745 | 3.871 | 1.150 |
| 3.5 | 9500 | 0.050 | 4.325 | 4.364 | 1.320 |

### *6.4. Calibration of the Process Damping Characteristics*

Figure 11 illustrates the variation in calibrated process damping coefficient $C_{pd}$ with axial depth of cut under different feed per tooth conditions at spindle speeds of 5500, 7500, and 9500 rpm. Smooth curves are obtained using shape-preserving interpolation, while markers represent calibrated data points. The damping coefficient was calibrated at values between $4.7 \times 10^9$ and $2.9 \times 10^{11}$ N/m$^2$ for cutting parameters specified in machining tests. The results indicate that process damping decreases with increasing axial depth of cut due to the gradual reduction in effective flank contact effects during high-speed machining [36,47]. In contrast, a smaller feed per tooth leads to stronger indentation and ploughing effects, resulting in larger effective damping coefficients. In addition, the effective damping coefficient was calculated from the calibrated process damping coefficients according to Equation (3) $C_{eff} = C_{pd} a_p f_z / V_c$. The effective damping coefficient is estimated to be in the range of 120–720 Ns/m, 180–900 Ns/m and 250–1100 Ns/m for a spindle speed of 5500, 7500 and 9500 rpm, respectively. Overall, the $C_{eff}$ falls within the range of approximately $10^2$–$10^3$ Ns/m, which is consistent with damping levels commonly

observed in milling operation [47,48]. This further confirms the physical plausibility of the identified process damping coefficients.

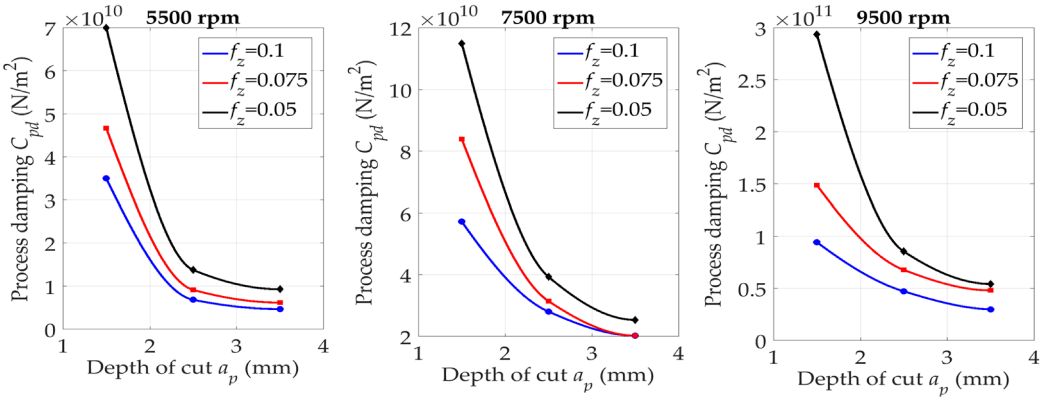


**Figure 11.** Variation in calibrated process damping coefficient $C_{pd}$ with axial depth of cut under different feed rates and spindle speeds.

Based on the calibrated process damping coefficients obtained from vibration matching between simulation and experiments, a parametric model was developed to describe the variation in process damping with axial depth of cut and spindle speed. To isolate the influence of feed per tooth, a normalized damping parameter was first introduced as

$$\Gamma(a_p, n) = C_{pd}(a_p, f_z, n)\, a_p f_z \tag{15}$$

where $C_{pd}$ is the process damping coefficient, $a_p$ is the axial depth of cut, $f_z$ is the feed per tooth, and $n$ is the spindle speed. This normalization allows the variation in process damping to be primarily characterized as a function of axial depth and spindle speed.

Analysis of the calibrated data indicated that the normalized parameter $\Gamma$ exhibits a depth-dependent saturation behavior. Accordingly, an exponential saturation model was adopted for each spindle speed node:

$$\Gamma(a_p \mid n_k) = A_k + B_k \exp\left(\frac{a_p}{a_{0,k}}\right) \tag{16}$$

where $A_k$, $B_k$, and $a_{0,k}$ are fitting parameters associated with spindle speed $n_k$. The parameter $A_k$ represents the asymptotic value of $\Gamma$ at large cutting depths, $B_k$ characterizes the additional damping contribution at shallow immersion, and $a_{0,k}$ denotes the characteristic depth controlling the saturation rate.

Based on the calibrated process damping data, a piecewise-by-speed exponential saturation model was derived, as illustrated in Figure 12. A normalized parameter $\Gamma(a_p, n) = C_{pd}(a_p, f_z, n) a_p f_z$ was first introduced to separate the feed effect from the damping coefficient. For each spindle speed, $\Gamma$ was fitted as an exponential function of axial depth of cut.

For $n = 5500$ rpm,

$$\Gamma(a_p \mid 5500) = 2.10 \times 10^3 + 6.10 \times 10^5 \exp\left(\frac{-a_p}{0.42}\right) \tag{17}$$

For $n = 7500$ rpm,

$$\Gamma(a_p \mid 7500) = 6.20 \times 10^3 + 1.25 \times 10^5 \exp\left(\frac{-a_p}{0.50}\right) \tag{18}$$

For $n = 9500$ rpm,

$$\Gamma(a_p \mid 9500) = 1.20 \times 10^4 + 3.10 \times 10^5 \exp\left(\frac{-a_p}{0.46}\right) \tag{19}$$

where $a_p$ is expressed in millimeters.

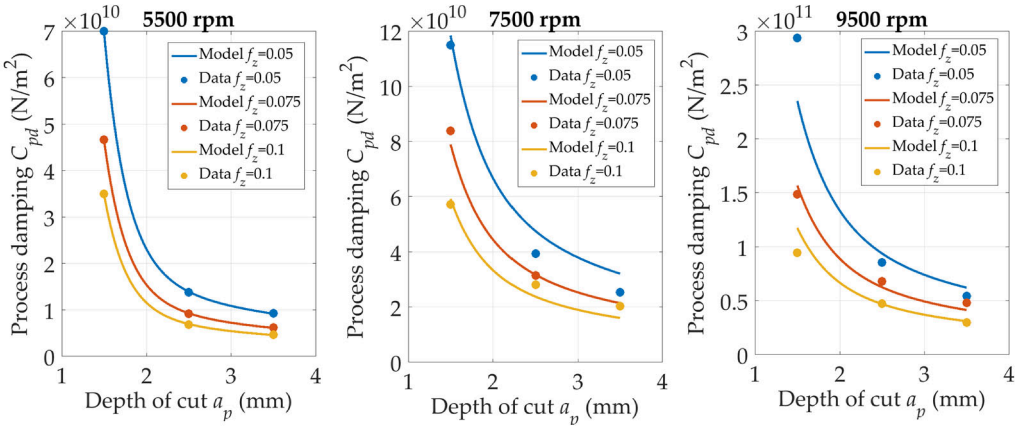


**Figure 12.** The fitted model of the calibrated process damping coefficients.

The process damping coefficient can therefore be expressed explicitly as

$$C_{pd}(a_p, f_z, n) = \frac{\Gamma(a_p, n)}{a_p f_z} \tag{20}$$

For spindle speeds between the calibrated nodes, the parameters $A(n)$, $B(n)$, and $a_0(n)$ are obtained through linear interpolation between the fitted values. The general form of the process damping model used in the digital twin simulation becomes

$$C_{pd}(a_p, f_z, n) = \frac{A(n) + B(n)\exp\left(\frac{a_p}{a_0(n)}\right)}{a_p f_z} \tag{21}$$

This explicit parametric formulation enables the process damping coefficient to be estimated for a wide range of cutting conditions without performing individual calibration for each machining test.

The agreement between the calibrated process damping coefficients and the fitted model was quantitatively evaluated using the mean absolute percentage error (MAPE) and root mean square error (RMSE). The results show that the proposed exponential model predicts the calibrated damping coefficients with good accuracy. The MAPE values for spindle speeds of 5500, 7500, and 9500 rpm are approximately 1.05%, 11.36%, and 11.11%, respectively, with corresponding RMSE values on the order of $10^8$–$10^9$ N/m$^2$. The overall average MAPE is about 12%, indicating that the proposed model adequately captures the variation in process damping with axial depth of cut and spindle speed. The model therefore provides a practical and physically reasonable approach for incorporating process damping into the digital twin simulation of milling dynamics.

### *6.5. Validation of the DT Model*

The digital twin model of the milling system was validated by using the dataset collected from second experimental phase. The validation dataset is listed in Table 4. Again, the machining vibrations under different conditions were predicted via the DT model and compared with the measured values, as shown in Figure 13. The coefficient of

determination between measured and predicted vibrations within the validation dataset is approximately $R^2 = 0.9283$.

**Table 4.** Dataset for DT validation.

| Cutting Depth, ap (mm) | Spindle Speed, s (rpm) | Feed, fz (mm/Tooth) | Measured Vibration (g) | Predicted Vibration (g) | Roughness, Ra (μm) |
|---|---|---|---|---|---|
| 1.00 | 3000 | 0.100 | 0.966 | 0.954 | 0.937 |
| 1.50 | 3000 | 0.100 | 1.207 | 1.440 | 1.044 |
| 2.00 | 3000 | 0.100 | 1.303 | 1.935 | 1.241 |
| 2.50 | 3000 | 0.100 | 1.609 | 2.448 | 1.314 |
| 3.00 | 3000 | 0.100 | 1.790 | 2.925 | 1.602 |
| 1.00 | 4000 | 0.100 | 1.448 | 0.959 | 1.126 |
| 1.50 | 4000 | 0.100 | 1.939 | 1.664 | 1.488 |
| 2.00 | 4000 | 0.100 | 2.354 | 2.219 | 1.734 |
| 2.50 | 4000 | 0.100 | 2.548 | 2.788 | 1.876 |
| 3.00 | 4000 | 0.100 | 2.685 | 3.352 | 1.979 |
| 1.00 | 6000 | 0.075 | 0.936 | 0.886 | 0.708 |
| 1.50 | 6000 | 0.075 | 1.469 | 1.468 | 0.978 |
| 2.00 | 6000 | 0.075 | 1.756 | 1.773 | 1.123 |
| 2.50 | 6000 | 0.075 | 2.016 | 2.212 | 1.227 |
| 3.00 | 6000 | 0.075 | 2.385 | 2.651 | 1.421 |
| 1.00 | 6000 | 0.050 | 0.781 | 0.962 | 0.867 |
| 1.50 | 6000 | 0.050 | 1.122 | 1.150 | 0.876 |
| 2.00 | 6000 | 0.050 | 1.244 | 1.399 | 1.005 |
| 2.50 | 6000 | 0.050 | 1.412 | 1.696 | 1.129 |
| 3.00 | 6000 | 0.050 | 1.690 | 2.016 | 1.261 |
| 2.00 | 7500 | 0.075 | 4.790 | 4.720 | 1.582 |
| 3.00 | 7500 | 0.075 | 5.600 | 5.279 | 2.099 |
| 4.00 | 7500 | 0.075 | 5.410 | 5.268 | 2.294 |
| 1.50 | 8500 | 0.050 | 2.600 | 2.158 | 0.861 |
| 2.50 | 8500 | 0.050 | 3.310 | 3.147 | 0.943 |
| 3.50 | 8500 | 0.050 | 4.070 | 4.111 | 1.057 |
| 2.00 | 9500 | 0.050 | 2.912 | 2.712 | 1.083 |
| 3.00 | 9500 | 0.050 | 3.458 | 3.489 | 1.574 |
| 4.00 | 9500 | 0.050 | 4.547 | 4.432 | 1.791 |

Within all datasets, including the training phase and validation phase, the coefficient of determination is $R^2 = 0.94$, and the overall MAPE and RMSE are about 10.39% and 0.234, respectively. This revealed that good agreement between the simulation and the experiment was achieved. Overall, the digital twin model successfully duplicates the variation in vibration levels with changing cutting conditions. The predicted vibration amplitudes follow the same trend as the experimental measurements, indicating that the dynamic interaction between the structural system and the cutting process is properly described in the model. It is observed that larger deviations were observed under certain cutting conditions, particularly at lower spindle speeds (3000 rpm). This can be attributed to the estimation of process damping at lower speed being beyond the fitted range of the calibrated

model derived from higher speed ranges. Essentially, the overall prediction accuracy remains satisfactory. The results confirm that the proposed digital twin model incorporated with the calibrated formulation of process damping characteristics is capable of reliably predicting the vibration response of the milling system. Consequently, DT-generated vibration can serve as a reliable virtual sensing input for surface quality modeling.

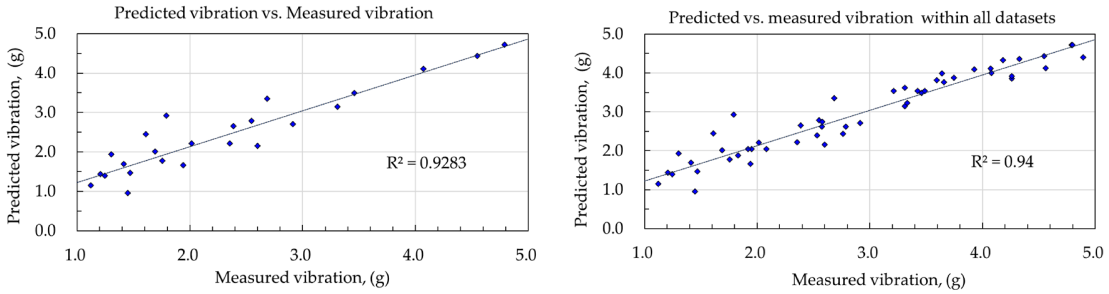


(**a**) (**b**)

**Figure 13.** Correlation between measured and predicted vibration (**a**) within the validation dataset and (**b**) within all datasets.

### *6.6. Application of Digital Twin Model Surface Roughness Prediction*

In addition to predicting the dynamic vibration behavior of the milling process, the developed digital twin model was further utilized for surface roughness prediction. In milling operations, surface quality is strongly influenced by the dynamic interaction between the cutting tool and the workpiece. Excessive tool vibration during machining can lead to irregular surface profiles and increased roughness. Therefore, vibration features can serve as effective indicators for predicting surface quality.

(a) Machining vibration vs. surface roughness

Figure 14 shows the relationship between surface roughness and vibration level for all datasets collected from machining tests. The scatter plot reveals a moderate positive correlation between measured vibration and surface roughness, with a coefficient of determination ($R^2$) of 0.386. This indicates that vibration amplitude is a factor influencing the surface generation during milling, while it only accounts for about 39% of the total variance. This implies that other process parameters also play a substantial role in determining the final surface quality. The correlation between measured roughness and DT-predicted vibration was evaluated with $R^2$ = 0.4724, which is comparable to the correlation of the measured vibration. This is a significant improvement (about 8.6% higher) over the measured vibration model ($R^2$ = 0.386). This result demonstrates that the DT-predicted vibration successfully preserves the key dynamic features that influence surface generation.

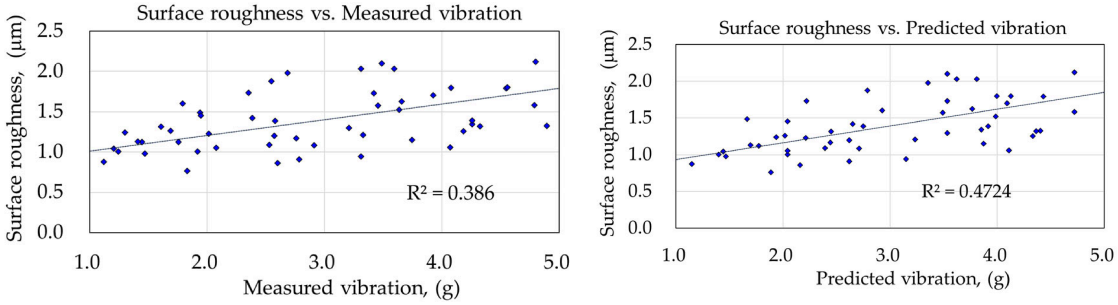


(**a**) (**b**)

**Figure 14.** Correlation between measured roughness and machining vibration. (**a**) Measured vibration; (**b**) predicted vibration.

The result also confirms that incorporating vibration features into surface roughness modeling is physically justified. Despite moderate absolute prediction errors in vibration amplitude at lower speed, the relative variation trend across cutting conditions is accurately captured. Consequently, DT-generated vibration seems to have a more consistent linear relationship with the resulting surface quality than the raw sensor data.

(b) Establishment of the surface roughness prediction model

In this study, a surface roughness prediction model was established by incorporating vibration features obtained from the digital twin simulation together with the cutting parameters. Specifically, the root mean square (RMS) vibration amplitude predicted by the digital twin model was used as an additional input variable for the roughness prediction model. The input variables of the model include spindle speed $n$, axial depth of cut $a_p$, feed per tooth $f_z$, and the predicted vibration feature $V_b$.

A regression-based prediction model was constructed to establish the relationship between these input variables and the resulting surface roughness $R_a$:

$$R_a = f(n, a_p, f_z, V_b) \tag{22}$$

where $R_a$ represents the arithmetic average surface roughness of the machined surface. Cutting parameters and tool vibration served as input variables. The vibration input was considered in two scenarios: measured vibration features and DT-predicted vibration features. Based on prior work [19], a power-law function was adopted to model the relationship between surface roughness and input variables:

$$R_a = \beta_0 \cdot {a_p}^{\beta 1} \cdot \mathrm{S}^{\beta 2} \cdot {f_z}^{\beta 3} \cdot {V_b}^{\beta 4} \tag{23}$$

where $V_b$ represents vibration features. Logarithmic transformation was applied to enable linear regression fitting. The regression coefficients were estimated using least-squares analysis. Two models were constructed:

(1) $R_a$ model based on measured vibration:

$$R_a = 1.216292 \cdot \left( a_p^{0.389456} \times \mathrm{S}^{0.004973} \times f_z^{0.551936} \times {V_{bm}}^{0.173492} \right) \tag{24}$$

(2) $R_a$ model based on DT-predicted vibration:

$$R_a = 0.871297 \cdot \left( a_p^{0.378252} \times \mathrm{S}^{0.047976} \times f_z^{0.558458} \times {V_{DT}}^{0.162903} \right) \tag{25}$$

Figure 15 presents a comparison of the observed surface roughness against the values predicted by the regression models. The coefficient of determination between the predicted and measured roughness is approximately 0.84 for both models, irrespective of whether the experimentally measured vibration data or digital twin (DT)-predicted vibration data served as the input variable. For the surface roughness model with measured vibration signals, the mean absolute percentage error (MAPE) and the root mean square error (RMSE) are 9.59% and 0.158 μm, respectively. Similarly, the roughness model driven by DT-predicted vibration features yielded comparable results, with an MAPE of 9.57% and an RMSE of 0.160 μm.

For describing the model accuracy, we have illustrated the distribution of prediction error in terms of the residual histograms based on the predictions of the two models, as shown in Figure 16. It is noted that model 1 shows a staggered distribution with a high frequency peak around −0.1 but then stays relatively flat across the 0 to 0.1 range before tapering off. For model 2, the histogram shows a much clearer Gaussian distribution with

a distinct central peak centered almost exactly at zero. This suggests that model 2 provides more consistent and reliable predictions for RA values. Overall, the higher frequency of near-zero errors in the residual histogram confirms that the enhanced precision makes the predictive model a reliable choice for consistent predictions across the observed range.

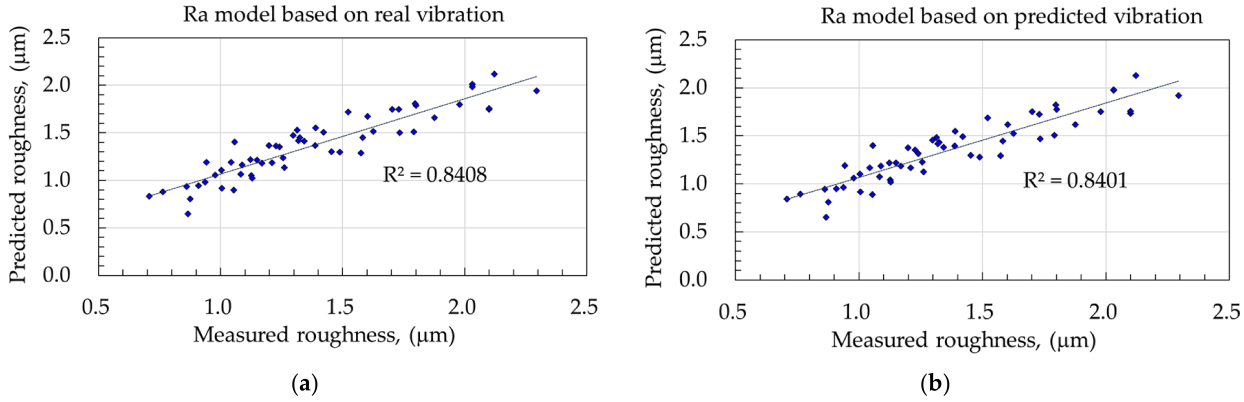


(**a**) (**b**)

**Figure 15.** Correlation of the measured roughness and predicted roughness. (**a**) Ra model based on measured vibration features; (**b**) Ra model based on DT-predicted vibration features.

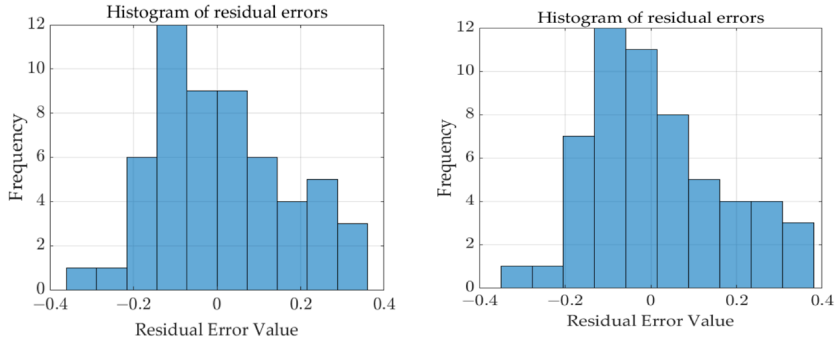


(**a**) (**b**)

**Figure 16.** Residual histograms of the prediction errors of surface roughness. (**a**) Predictive model based on measured vibration; (**b**) predictive model based on predicted vibration.

### *6.7. Discussions*

As demonstrated in Figure 15, the results indicate that the two models exhibit comparable predictive performance, each achieving an overall prediction accuracy of approximately 90%. The slight difference observed between the models implies that the vibration characteristics generated by the digital twin can effectively replace experimentally obtained vibration signals in forecasting surface roughness. As a result, this finding supports the feasibility of the digital twin model as a virtual sensing platform, enabling reliable surface quality predictions without the need for direct vibration measurements during the machining process.

However, it should be emphasized that the machining vibration is influenced not only by cutting parameters but also by multiple time-varying and nonlinear factors, which include tool geometry and wear progression of the cutting edge, machining resistance of the material, and variations in the real contact state between the cutting edge and the workpiece [34,36]. In practical machining operations, these factors introduce uncertainty into the dynamic cutting process and may alter the effective damping capability of the milling system and hence the anti-vibration capability in machining operation due to process damping effects [49–51].

On the other hand, machining vibration prediction can also be investigated by using regression-based and ANN-based data-driven models derived from experimentally measured datasets [19]. Although these approaches provided acceptable prediction accuracy, their predictive capability strongly depended on the quality and coverage of the training data, and the resulting models offered limited physical interpretability. Compared with these purely data-driven approaches, the digital twin model presented in this study adopts a physics-informed two-degree-of-freedom representation of a milling system based on experimentally identified modal parameters with a mechanistic cutting force model. This approach effectively reproduces the dominant structural vibration mode, while the higher-order modes and nonlinear contact effects are not explicitly modeled.

By incorporating the physical characteristics of the machining system, the proposed framework reduces reliance on extensive experimental datasets while enabling direct prediction of machining vibration responses under varying cutting conditions. Consequently, a small deviation between predicted and measured vibration amplitudes (MAPE = 10.39%, RMSE = 0.234) was observed within all the datasets. Such deviation is considered acceptable given the inherent complexity of milling dynamics and the simplified modeling framework. The coefficient of determination between measured and predicted vibration amplitudes is approximately $R^2 = 0.94$, indicating consistent predictive performance.

A key advantage of the proposed digital twin framework lies in its capability for parameter calibration and updating. Since the structural modal parameters are experimentally identifiable, the digital twin can be recalibrated through periodic impact testing or operational modal analysis. In addition, cutting force coefficients and process damping parameters may be updated using measured vibration data during machining. The exponential saturation form adopted for the normalized damping parameter $\Gamma(a_p, n)$ reflects the physical characteristics of tool–workpiece contact during dynamic milling. When the axial depth of cut is small, the contact between the tool flank face and the previously machined surface occurs over a relatively short contact length. Under these conditions, the indentation and rubbing effects of the flank face are more sensitive to small changes in cutting depth. This will result in a relatively large variation in the effective damping contribution. This behavior is represented by the model in exponential form, which shows a strong dependence of process damping on cutting depth. In addition, the calibrated process damping coefficients obtained in this study fall within the range reported in previous machining dynamics investigations. Although the identified coefficients appear relatively large, the effective damping contribution in the dynamic model is determined by the term $C_{pd} a_p f_z / V_c$, which yields damping levels on the order of $10^2$–$10^3$ Ns/m. These values are consistent with experimentally identified damping levels reported in the literature for milling processes under low-chip-thickness conditions [34,36].

As the axial depth of cut increases, the effective contact region between the tool flank and the workpiece surface gradually approaches a stable condition. In this regime, further increases in cutting depth produce only minor changes in the contact mechanics, and therefore the damping contribution tends to approach a constant value. In the calibrated damping formula, Equation (15), this asymptotic behavior is represented by the parameter $A_k$, which corresponds to the saturation level of the normalized damping parameter at larger depths of cut. The parameter $B_k$ quantifies the additional damping contribution, which is most prominent at small immersion depths. In contrast, the characteristic depth parameter $a_{0,k}$ governs the rate at which the transition from the shallow-depth domain to the saturation regime unfolds. The influence of spindle speed on these parameters underestimates the impact of cutting velocity on both the contact duration between the cutting edge and the workpiece and the frictional interactions during dynamic cutting processes.

Therefore, although the proposed model is derived from calibrated experimental data, its mathematical form is consistent with the underlying physical mechanisms of process damping in milling operations. Future improvement of the DT model could be achieved by taking the progression of tool wear and adaptive identification algorithms of system dynamic parameters into consideration to improve the reliability of long-term predictions. Moreover, the capability of monitoring machining performance in real time and quality control can be further strengthened by incorporating online parameter updating strategies in the evolution of the digital twin modeling framework.

## 7. Conclusions

This study proposed a physics-based digital twin (DT) model for milling operation. The model combined structural dynamic properties with a mechanistic cutting force model. By integrating experimentally identified modal parameters, shear and edge force components, and a calibrated process damping model, the framework provides a unified time-domain simulation environment.

To ensure the model is suitable for different cutting conditions, we developed a structured calibration methodology to identify the process damping coefficients by minimizing the error between predicted and measured vibration amplitudes. A key contribution of this approach is the introduction of a normalized damping parameter into an exponential depth-dependent saturation function, which can further be utilized to estimate the process damping coefficient for varying conditions. The reliability of the digital twin was confirmed through extensive validation, which shows the model can predict vibration responses across different cutting parameters with an average error of approximately 10%. It was verified that the calibrated process damping model can successfully capture the overall variation trend of damping behavior with axial depth of cut and spindle speed.

In addition, a surface roughness prediction model was established by incorporating the cutting parameters and vibration features obtained from the digital twin simulation. The average prediction accuracy across all datasets is approximately 91%, which is comparable to that achieved using models based on measured vibration features. This result indicates that, within the investigated cutting conditions, the digital-twin-predicted vibration features can serve as an effective input for surface roughness prediction, demonstrating its potential as a virtual sensing approach. Beyond its predictive capability, the proposed digital twin framework also provides a physically interpretable and standardized methodology for machining process monitoring, virtual sensing, and future adaptive quality control applications in intelligent manufacturing environments.

**Author Contributions:** Conceptualization and methodology, M.A.R., W.-Z.L. and J.-P.H.; software and formal analysis, M.A.R., W.-Z.L., Y.-S.L. and Z.-M.S.; investigation, M.A.R., W.-Z.L., Y.-S.L. and Z.-M.S.; resources, J.-P.H.; data curation, M.A.R., W.-Z.L., Y.-S.L. and Z.-M.S.; writing—original draft preparation, M.A.R., W.-Z.L., Y.-S.L. and J.-P.H.; writing—review and editing, J.-P.H.; visualization, M.A.R. and W.-Z.L.; supervision, J.-P.H.; project administration, J.-P.H.; funding acquisition, J.-P.H. All authors have read and agreed to the published version of the manuscript.

**Funding:** This research was funded by the National Science and Technology Council, Taiwan, under grant number NSTC 111-2221-167-021.

**Data Availability Statement:** The data is contained within this article.

**Conflicts of Interest:** The authors declare no conflicts of interest.

## References


1. Lee, J.; Lapira, E.; Bagheri, B.; Kao, H.A. Recent advances and trends in predictive manufacturing systems in big data environment. *Manuf. Lett.* **2013**, *1*, 38–41. [CrossRef]
2. Lee, D.; Kim, C.K.; Yang, J.; Cho, K.Y.; Choi, J.; Noh, S.D.; Nam, S. Digital twin-based analysis and optimization for design and planning of production lines. *Machines* **2022**, *10*, 1147. [CrossRef]
3. Lim, K.Y.H.; Zheng, P.; Chen, C.H. A state-of-the-art survey of Digital Twin: Techniques, engineering product lifecycle management and business innovation perspectives. *J. Intell. Manuf.* **2020**, *31*, 1313–1337. [CrossRef]
4. Grieves, M.; Vickers, J. Digital twin: Mitigating unpredictable, undesirable emergent behavior in complex systems. In *Transdisciplinary Perspectives on Complex Systems: New Findings and Approaches*; Springer International Publishing: Cham, Switzerland, 2016; pp. 85–113.
5. Kabir, M.R.; Ray, S. Digital Twin Tools for Smart Manufacturing: A Paradigm Shift for Industry 4.0. *IEEE Open J. Ind. Electron. Soc.* **2025**, *6*, 1756–1770. [CrossRef]
6. Li, J.; Yan, W.; Zhang, M.; Zhu, S.; Jiang, Z.; Fan, Z. Digital twin-based multi-view energy efficiency prediction for machining systems. *Digit. Twin* **2026**, 2634493. [CrossRef]
7. Lim, K.Y.H.; Zheng, P.; Chen, C.H.; Huang, L. A digital twin-enhanced system for engineering product family design and optimization. *J. Manuf. Syst.* **2020**, *57*, 82–93. [CrossRef]
8. Fu, Y.; Zhu, G.; Zhu, M.; Xuan, F. Digital twin for integration of design-manufacturing-maintenance: An overview. *Chin. J. Mech. Eng.* **2022**, *35*, 80. [CrossRef]
9. Ding, K.; Chan, F.T.; Zhang, X.; Zhou, G.; Zhang, F. Defining a digital twin-based cyber-physical production system for autonomous manufacturing in smart shop floors. *Int. J. Prod. Res.* **2019**, *57*, 6315–6334. [CrossRef]
10. Tao, F.; Cheng, J.; Qi, Q.; Zhang, M.; Zhang, H.; Sui, F. Digital twin-driven product design, manufacturing and service with big data. *Int. J. Adv. Manuf. Technol.* **2018**, *94*, 3563–3576. [CrossRef]
11. Hänel, A.; Schnellhardt, T.; Wenkler, E.; Nestler, A.; Brosius, A.; Corinth, C.; Fay, A.; Ihlenfeldt, S. The development of a digital twin for machining processes for the application in aerospace industry. *Procedia CIRP* **2020**, *93*, 1399–1404. [CrossRef]
12. Cai, Y.; Starly, B.; Cohen, P.; Lee, Y.S. Sensor data and information fusion to construct digital-twins virtual machine tools for cyber-physical manufacturing. *Procedia Manuf.* **2017**, *10*, 1031–1042. [CrossRef]
13. Liu, J.; Wen, X.; Zhou, H.; Sheng, S.; Zhao, P.; Liu, X.; Kang, C.; Chen, Y. Digital twin-enabled machining process modeling. *Adv. Eng. Inform.* **2022**, *54*, 101737. [CrossRef]
14. Liu, M.; Fang, S.; Dong, H.; Xu, C. Review of digital twin about concepts, technologies, and industrial applications. *J. Manuf. Syst.* **2021**, *58*, 346–361. [CrossRef]
15. Tao, F.; Zhang, M.; Cheng, J.; Qi, Q. Digital twin workshop: A new paradigm for future workshop. *Comput. Integr. Manuf. Syst.* **2017**, *23*, 1–9.
16. Tao, F.; Liu, W.; Zhang, M.; Hu, T.L.; Qi, Q.; Zhang, H.; Sui, F.; Wang, T.; Xu, H.; Huang, Z.; et al. Five-dimension digital twin model and its ten applications. *Comput. Integr. Manuf. Syst.* **2019**, *25*, 1–18.
17. Bakhshandeh, P.; Mohammadi, Y.; Altintas, Y.; Bleicher, F. Digital twin assisted intelligent machining process monitoring and control. *CIRP J. Manuf. Sci. Technol.* **2024**, *49*, 180–190. [CrossRef]
18. Fu, X.; Song, H.; Li, S.; Lu, Y. Digital twin technology in modern machining: A comprehensive review of research on machining errors. *J. Manuf. Syst.* **2025**, *79*, 134–161. [CrossRef]
19. Lin, Y.C.; Wu, K.D.; Shih, W.C.; Hsu, P.K.; Hung, J.P. Prediction of surface roughness based on cutting parameters and machining vibration in end milling using regression method and artificial neural network. *Appl. Sci.* **2020**, *10*, 3941. [CrossRef]
20. Qiu, Y.; Mao, X.; Gao, C.; Xu, Y.; Liu, H. Structural dynamics-driven digital twin framework for real-time vibration modelling of machine tools. *Mech. Syst. Signal Process.* **2025**, *240*, 113406. [CrossRef]
21. Tseng, T.L.; Konada, U.; Kwon, Y. A novel approach to predict surface roughness in machining using fuzzy theory. *J. Comput. Des. Eng.* **2016**, *3*, 1–13. [CrossRef]
22. Cus, F.; Zuperl, U. Approach to optimization of cutting conditions by using artificial neural networks. *J. Mater. Process. Technol.* **2006**, *173*, 281–290. [CrossRef]
23. Oktem, H.; Erzurumlu, T.; Erzincanli, F. Prediction of minimum surface roughness in end milling mold parts using neural network and genetic algorithm. *Mater. Des.* **2006**, *27*, 735–744. [CrossRef]
24. Wang, Q.; Wang, H.; Hou, L.; Yi, S. Overview of Tool Wear Monitoring Methods Based on Convolutional Neural Network. *Appl. Sci.* **2021**, *11*, 12041. [CrossRef]
25. Zhuang, K.; Shi, Z.; Sun, Y.; Gao, Z.G.; Wang, L. Digital twin-driven tool wear monitoring and predicting method for the turning process. *Symmetry* **2021**, *13*, 1438. [CrossRef]
26. Liu, X.; Li, X.; Ding, M.; Yue, C.; Wang, L.; Liang, Y.; Zhang, B. Intelligent management and control technology of cutting tool life-cycle for intelligent manufacturing. *J. Mech. Eng.* **2021**, *57*, 196–219.

27. Zi, X.; Gao, S.; Xie, Y. An online monitoring method of milling cutter wear condition driven by digital twin. *Sci. Rep.* **2024**, *14*, 4956. [CrossRef]
28. Liu, X.; Cheng, K. Modelling the machining dynamics of peripheral milling. *Int. J. Mach. Tools Manuf.* **2005**, *45*, 1301–1320. [CrossRef]
29. Zagórski, I.; Kulisz, M.; Semeniuk, A.; Malec, A. Artificial neural network modeling of vibration in the milling of AZ91D alloy. *Adv. Sci. Technol. Res. J.* **2017**, *11*, 261–269. [CrossRef]
30. Chen, Y.; Sun, R.; Gao, Y.; Leopold, J. A nested-ANN prediction model for surface roughness considering the effects of cutting forces and tool vibrations. *Measurement* **2017**, *98*, 25–34. [CrossRef]
31. Qiao, Q.; Wang, J.; Ye, L.; Gao, R.X. Digital twin for machining tool condition prediction. *Procedia CIRP* **2019**, *81*, 1388–1393. [CrossRef]
32. Zhao, P.; Sun, B. Adaptive modification of digital twin model of CNC machine tools coordinately driven by mechanism model and data model. *J. Phys. Conf. Ser.* **2021**, *1875*, 012003. [CrossRef]
33. Altintas, Y.; Eynian, M.; Onozuka, H. Identification of dynamic cutting force coefficients and chatter stability with process damping. *CIRP Ann. Manuf. Technol.* **2008**, *57*, 371–374. [CrossRef]
34. Altintas, Y.; Weck, M. Chatter stability of metal cutting and grinding. *CIRP Ann. Manuf. Technol.* **2004**, *53*, 619–642. [CrossRef]
35. Das, M.K.; Tobias, S.A. The relation between the static and the dynamic cutting of metals. *Int. J. Mach. Tool Des. Res.* **1967**, *7*, 63–89. [CrossRef]
36. Tunç, L.T.; Budak, E. Effect of cutting conditions and tool geometry on process damping in machining. *Int. J. Mach. Tools Manuf.* **2012**, *57*, 10–19. [CrossRef]
37. Taylor, C.M.; Sims, N.D.; Turner, S. Process damping and cutting tool geometry in machining. *IOP Conf. Ser. Mater. Sci. Eng.* **2011**, *26*, 012009. [CrossRef]
38. Chiou, R.Y.; Liang, S.Y. Chatter stability of a slender cutting tool in turning with tool wear effect. *Int. J. Mach. Tools Manuf.* **1998**, *38*, 315–327. [CrossRef]
39. Clancy, B.E.; Shin, Y.C. A comprehensive chatter prediction model for face turning operation including tool wear effect. *Int. J. Mach. Tools Manuf.* **2002**, *42*, 1035–1044. [CrossRef]
40. Yan, W.; Wong, Y.S.; Lee, K.S.; Ning, T. An investigation of indices based on milling force for tool wear in milling. *J. Mater. Process. Technol.* **1999**, *89*, 245–253. [CrossRef]
41. Plaza, E.G.; López, P.N. Analysis of cutting force signals by wavelet packet transform for surface roughness monitoring in CNC turning. *Mech. Syst. Signal Process.* **2018**, *98*, 634–651. [CrossRef]
42. Yesilyurt, I.; Ozturk, H. Tool condition monitoring in milling using vibration analysis. *Int. J. Prod. Res.* **2007**, *45*, 1013–1028. [CrossRef]
43. Aslan, A. Optimization and analysis of process parameters for flank wear, cutting forces and vibration in turning of AISI 5140: A comprehensive study. *Measurement* **2020**, *163*, 107959. [CrossRef]
44. Afazov, S.; Scrimieri, D. Chatter model for enabling a digital twin in machining. *Int. J. Adv. Manuf. Technol.* **2020**, *110*, 2439–2444. [CrossRef]
45. Altintas, Y. *Manufacturing Automation: Metal Cutting Mechanics, Machine Tool Vibrations, and CNC Design*; Cambridge University Press: Cambridge, UK, 2000.
46. Tsai, M.Y.; Chang, S.Y.; Hung, J.P.; Wang, C.C. Investigation of milling cutting forces and cutting coefficient for aluminum 6060-T6. *Comput. Electr. Eng.* **2016**, *51*, 320–330. [CrossRef]
47. Tyler, C.T.; Schmitz, T.L. Analytical Process Damping Stability Prediction. *J. Manuf. Process.* **2013**, *15*, 69–76. [CrossRef]
48. Tunc, L.T.; Budak, E. Identification and Modeling of Process Damping in Milling. *J. Manuf. Sci. Eng.* **2013**, *135*, 021001. [CrossRef]
49. Li, M.; Zhao, W.; Li, L.; He, N.; Jamil, M. Chatter suppression during milling of Ti-6Al-4V based on variable pitch tool and process damping effect. *Machines* **2022**, *10*, 222. [CrossRef]
50. The Ho, Q.N.; Do, T.T.; Minh, P.S. Studying the factors affecting tool vibration and surface quality during turning through 3D cutting simulation and machine learning model. *Micromachines* **2023**, *14*, 1025. [CrossRef] [PubMed]
51. Mladjenovic, C.; Monkova, K.; Zivkovic, A.; Knezev, M.; Marinkovic, D.; Ilic, V. Experimental identification of milling process damping and its application in stability lobe diagrams. *Machines* **2025**, *13*, 96. [CrossRef]